arXiv:1409.2599v1 [stat.ME] 9 Sep 2014

Iterative Posterior Inference for Bayesian Kriging

Zepu Zhang

October 13, 2011

Abstract

We propose a method for estimating the posterior distribution of a standard geostatistical model. After choosing the model formulation and specifying a prior, we use normal mixture densities to approximate the posterior distribution. The approximation is improved iteratively. Some difficulties in estimating the normal mixture densities, including determining tuning parameters concerning bandwidth and localization, are addressed. The method is applicable to other model formulations as long as all the parameters, or transforms thereof, are defined on the whole real line, $(-\infty, \infty)$. Ad hoc treatments in the posterior inference such as imposing bounds on an unbounded parameter or discretizing a continuous parameter are avoided. The method is illustrated by two examples, one using digital elevation data and the other using historical soil moisture data. The examples in particular examine convergence of the approximate posterior distributions in the iterations.

Key Words: geostatistics; importance sampling; normal mixture; kernel density estimation; anisotropy; change of support

1 Introduction

In the geostatistical literature, likelihood-based methods for parameter estimation make explicit assumptions on the statistical distributions of the spatial variable in question, thus contrast with some traditional methods such as ones based on curve-fitting for an empirical variogram model [Kovitz and Christakos, 2004; Emery, 2007]. The distributional assumptions are manifested, for example, in "model-based geostatistics" [Diggle and Ribeiro Jr., 2007] and "trans-Gaussian" models [Christensen et al., 2001]. First employed apparently in the early 1980s, likelihood-based methods have by now established themselves as a standard approach [see Zimmerman, 2010, for a review].

Given the distributional assumptions, one may obtain maximum likelihood (ML) estimates of the parameters, such as parameters in the spatial covariance function. However, estimating an "optimal" value for the parameters of the covariance function via ML methods is flawed because, according to Warnes and Ripley [1987], the profile likelihood can be multimodal and is often nearly flat in the neighborhood of its mode. These problems suggest that ML estimates may be difficult to find and such estimates, if found, may not be truly "representative" or "optimal". Handcock and Stein [1993] further emphasize that "plug-in"

zepu.zhang@gmail.com
Department of Mathematics and Statistics, University of Alaska, Fairbanks, Alaska, USA

Published in `Stochastic Environmental Research and Risk Assessment`, 2011.
doi:10.1007/s00477-011-0544-y

measures of prediction uncertainty based on ML parameter estimates tend to be over optimistic. They argue that a Bayesian approach mitigates this problem. Indeed, parallel to the growth of Bayesian statistics in general, Bayesian geostatistics (or Bayesian kriging) has enjoyed steady growth since the 1980s [Kitanidis, 1986; Handcock and Stein, 1993; de Oliveira et al., 1997; Ecker and Gelfand, 1999; Berger et al., 2001; Diggle and Ribeiro Jr., 2002; Banerjee et al., 2004; Palacios and Steel, 2006; Cowles et al., 2009].

In this study, we take a typical geostatistical formulation and present an algorithm for deriving a numerical representation of the posterior distribution of the parameters. The parameter vector, θ, consists of standard elements such as trend coefficients β, variance η^2, scale λ, smoothness κ, etc. It also accommodates geometric anisotropy. The prior specification combines standard non-informative priors (for β and η^2) and informative priors (for λ and κ). The algorithm uses a normal mixture to approximate the posterior density; the approximation is updated iteratively to approach the true posterior distribution.

The proposed algorithm avoids two empirical treatments that have been used in the literature, namely, imposing bounds on an unbounded parameter and discretizing a continuous parameter. One parameter that has received such treatments is the scale parameter, λ [de Oliveira et al., 1997; Diggle and Ribeiro Jr., 2007, sec. 7.2; Cowles et al., 2009]. These treatments have conceptual as well as practical complications. Conceptually, one needs to take great care to defend one's subjectively chosen bounds for an unbounded parameter by showing that the posterior inference is not sensitive to these bounds [Berger et al., 2001]. Practically, discretizing a continuous parameter renders the computational cost directly proportional to the resolution of the discretization. If discretization and artificial bounds are applied simultaneously on one parameter, say the scale λ, the desires to use wide bounds and dense discretization exert great burden on computation. Furthermore, the discretization approach is not scalable, in the sense that the computational cost grows exponentially as the number of parameters being discretized increases.

The central step of the algorithm, multivariate kernel density estimation, is a standard task with unsolved difficulties [Silverman, 1986; Scott, 1992; Wand and Jones, 1995]. Our algorithm makes particular efforts to determine two tuning parameters, one concerning localization and the other concerning bandwidth, by a likelihood criterion. Another technical difficulty arises from high skewness of importance weights, especially in early iterations. This problem is alleviated by a "flattening" transform.

This study intends to provide a generic, or routine, procedure for the posterior inference of Bayesian kriging parameters. As already mentioned, the procedure specifies a prior with limited user intervention, improves an initial, rough approximation iteratively, and avoids some ad hoc treatments that have been used in the literature. Moreover, the procedure is readily applicable to other model formulations so long as all the model parameters are defined on $(-\infty, \infty)$ or can be transformed to be so. In this sense, application of the algorithm extends beyond geostatistics.

The article is organized as follows. The geostatistical parameterization for a spatial variable is described in Section 2, with details on the Matérn correlation function, geometric anisotropy, the likelihood function, and specification of the prior. The technical core of this article, the iterative algorithm for posterior inference, is the subject of Section 3. The proposed method is capable of dealing with a type of "change-of-support" problems; this is briefly discussed in Section 4. In Section 5, we apply the geostatistical model and the

algorithm in two examples, one using synthetic data and the other using historical data. Section 6 concludes the article with a summary.

2 Parameterization

Let $Y(x)$ be a spatial random variable, where $x \in \Omega \subset \mathcal{R}^d$ is location in d-dimensional space (hence x is a d-vector, $d = 1, 2, 3$). We adopt the following mixed-effects model for $Y(x)$:

$$Y(x) = \mu(x)^T\beta + \sqrt{1-\tau}\,\eta\,\varrho(x) + \sqrt{\tau}\eta\,\epsilon(x), \tag{1}$$

where $\mu(x)$ is a p-vector of deterministic covariates (e.g. polynomials of the spatial coordinates); β is a p-vector of trend coefficients; $\varrho(x)$ is a zero-mean, unit-variance, stationary Gaussian process; $\epsilon(x)$ is an iid standard normal white-noise process; $\eta > 0$ is the standard deviation of $Y(x)$; and $0 \le \tau < 1$ is a nugget parameter. The process $\varrho(x)$ is characterized by a correlation function parameterized by a q-vector ϕ. In addition, we assume $\varrho(x)$ and $\epsilon(x)$ are independent of each other.

We denote the full parameter vector by $\theta = (\beta, \tau, \eta^2, \phi)$. Modeling efforts are typically concentrated on inferencing and interpreting the nugget parameter τ, the variance η^2, and the correlation parameter(s) ϕ. The content of ϕ depends on the specific correlation function employed; our choice here is the Matérn correlation function, to be described below. In addition, the formulation above allows for geometric anisotropy, parameters of which are also contained in ϕ.

2.1 Correlation function

We assume spatial stationarity for Y, hence the correlation between $Y(x_1)$ and $Y(x_2)$ is a function of scaled distance, denoted by $\ell(x_1, x_2) = |x_1 - x_2|/\lambda$, where λ is the "scale" parameter.

The marginal distribution of $Y(x)$ in the formulation (1) is $N\big(\mu(x)^T\beta,\, \eta^2\big)$. Of the total variance η^2, $\tau\eta^2$ is contributed by the white noise component $\sqrt{\tau}\eta\,\epsilon(x)$, whereas the spatially correlated component $\sqrt{1-\tau}\eta\varrho(x)$ contributes a variance of $(1-\tau)\eta^2$. In other words, the so-called "nugget effect" accounts for a fraction τ of the total variance. The covariance between $Y(x_1)$ and $Y(x_2)$ is

$$\begin{aligned} \operatorname{cov}\big(Y(x_1), Y(x_2)\big) &= \eta^2 \operatorname{corr}\big(Y(x_1), Y(x_2)\big) \\ &= \eta^2\Big((1-\tau)\rho\big(\ell(x_1, x_2)\big) + \tau I(x_1 = x_2)\Big), \end{aligned} \tag{2}$$

where I is the identity function, assuming value 1 if x_1 coincides with x_2 and 0 otherwise, and ρ is taken to be the Matérn correlation function:

$$\rho(\ell; \kappa) = \frac{1}{2^{\kappa-1}\Gamma(\kappa)}\,\ell^\kappa\,\mathcal{K}_\kappa(\ell), \quad \kappa > 0, \tag{3}$$

where Γ is the gamma function, $\mathcal{K}_\kappa$ is the modified Bessel function of the third kind of order κ [Abramowitz and Stegun, 1965, secs 9.6 and 10.2]; and κ is the smoothness parameter [Stein, 1999, p. 31; Diggle and Ribeiro Jr., 2007, p. 51].

In summary, in a 1-D model or 2- and 3-D isotropic models, the correlation parameter ϕ contains two elements, λ and κ. In an anisotropic model, ϕ contains additional elements that characterize anisotropy, as we discuss next.

2.2 Geometric anisotropy

When $d > 1$, our formulation allows for geometric anisotropy. Zimmerman [1993] distinguishes three forms of geometric anisotropy, including anisotropy in sill, in range (the "scale" parameter here), and in nugget, respectively. Range anisotropy is the most commonly discussed and is also the anisotropy considered here. When such anisotropy is present, the scaled distance, ℓ, is calculated in a transformed coordinate system, which is obtained by rotating the "natural" axes to the major and minor directions of anisotropy, and using different scales (λ's) along different axes. Specifically, in 2-D we need one angle (α) and two scales (λ_1, λ_2) to describe such anisotropy, whereas in 3-D we need three angles (α_1, α_2, α_3) and three scales (λ_1, λ_2, λ_3). The rotational angles determine a transformation matrix, $\boldsymbol{A}$ [see, e.g. Wackernagel, 2003, p. 62]. With the matrix $\boldsymbol{A}$ and directional scales $\lambda_1, \ldots, \lambda_d$, define

$$\boldsymbol{B}(\lambda, \boldsymbol{A}) = \boldsymbol{A}[\mathrm{diag}(\lambda_1^{-2}, \ldots, \lambda_d^{-2})]\boldsymbol{A}^T,$$

where $\mathrm{diag}(\lambda_1^{-2}, \ldots, \lambda_d^{-2})$ denotes the diagonal matrix with $\lambda_1^{-2}, \ldots, \lambda_d^{-2}$ on the main diagonal. The scaled distance is then defined by

$$\ell(x_1, x_2) = \sqrt{[x_1 - x_2]^T \boldsymbol{B}\,[x_1 - x_2]}. \tag{4}$$

Note that the $x_1 - x_2$ is a column vector of length d. This ℓ is used in (3) to calculate ρ.

In a study of geometric anisotropy in 2-D, Ecker and Gelfand [1999] treat the matrix $\boldsymbol{B}$ as parameter and derive $\boldsymbol{A}$ and λ from $\boldsymbol{B}$. They discuss, in a Bayesian context, how to specify a prior for $\boldsymbol{B}$ using the Wishart distribution. The parameterization we adopt goes in the opposite direction. With our parameterization, priors for the angle(s) α and the scales λ are specified. This parameterization has some advantages in terms of interpretation and intuition. These two parameterizations contain the same number of unknowns. Hristopulos [2002] studies more general forms of anisotropy that are not considered here.

In summary, in a 2-D anisotropic model, the correlation parameter ϕ consists of elements κ, α, and λ_1, λ_2; in a 3-D anisotropic model, ϕ consists of κ, α_1, α_2, α_3, and λ_1, λ_2, λ_3.

2.3 Likelihood

The parameter vector is denoted by $\theta = (\beta, \tau, \eta^2, \phi)$. The content of the correlation parameter ϕ depends on the spatial dimension d and whether anisotropy is considered, as discussed above. Suppose we have measurements of Y, denoted by $\boldsymbol{y}$, at n locations $\boldsymbol{x}$. The likelihood function of θ with respect to $\boldsymbol{y}$ is equal to

$$p(\boldsymbol{y} \,|\, \theta) = (2\pi\eta^2)^{-n/2}\, |\boldsymbol{R}|^{-1/2} \exp\Big(-\frac{1}{2\eta^2}\big(\boldsymbol{y} - \boldsymbol{X}\beta\big)^T \boldsymbol{R}^{-1}\big(\boldsymbol{y} - \boldsymbol{X}\beta\big)\Big), \tag{5}$$

where $\boldsymbol{X}$ is the "design matrix" of covariates corresponding to $\boldsymbol{x}$, each row being $\mu(x)$ for a single location x; $\boldsymbol{R}$ is the correlation matrix between the locations $\boldsymbol{x}$, calculated using the relations (2) and (3).

In applications, the parameter vector θ could be simplified depending on the actual situation of the spatial variable and emphasis of the investigation. For example, one might choose to fix the smoothness κ at a certain value, say 0.5 or 1.5. (Then, κ would not appear in

θ.) For another example, one might decide, based on background knowledge, not to consider anisotropy, hence λ would be a scalar, and ϕ would not contain α.

When anisotropy is considered, the coordinate rotation affects location-aware calculations including the trend function (via $\mu(x)$ and β) and the correlation. We choose to define the trend function in terms of the original coordinates. The angles (α's) define the rotations; the scales (λ's) are applied along the axes after the rotation. The parameters κ, τ, and η^2 do not have directional components because we consider range anisotropy only.

2.4 Specification of prior

We specify a prior with independent components:

$$\pi(\beta, \eta^2, \tau, \lambda, \kappa, \alpha) = \left(\eta^2\right)^{-1} \text{beta}(\tau; \cdot)\ \text{gamma}(\lambda; \cdot)\ \text{gamma}(\kappa; \cdot)\ \text{unif}(\alpha; 0, \pi/2). \tag{6}$$

(Remember that α appears in anisotropic models only. In anisotropic models, λ contains, and α may contain, more than one elements.) This specifies a flat prior on $(-\infty, \infty)$ for the trend coefficients β and a conventional noninformative prior for the variance η^2. It is sensible to use a diffuse prior for λ, whereas subjective information (or preference) about κ and τ may be injected into their priors. Relevant discussions can be found in Berger et al. [2001], Banerjee et al. [2004, sec. 5.1.1], Gelman et al. [2004, p. 50], and Gelman [2006]. Additional parameters need to be chosen for the beta and gamma distributions. Some details are listed below. However, bear in mind that these particularities are empirical and subject to adjustment.

beta$(\tau; \cdot)$: this is taken to be beta$(\tau; 1, 5) = (1-\tau)^4 I(0 \le \tau \le 1)$. This prior places more weight on small nugget values.

gamma$(\lambda; \cdot)$: this is taken to be gamma$(\lambda; 1, L/(2 \log 2))$, where L is the size of the model domain. This is actually the exponential distribution with median $L/2$.

gamma$(\kappa; \cdot)$: parameters of this gamma distribution are chosen such that its mode is 1.5 and its variance is 4.0.

3 Inference of the posterior

We estimate the posterior distribution of the parameter vector, θ, by normal mixtures in an iterative procedure. The versatility of normal mixtures in approximating complex densities is documented by Marron and Wand [1992]. The normal kernel implies that all components of θ must be defined on $(-\infty, \infty)$. This requires that the support of each component of θ is one of $(-\infty, \infty)$, (c, ∞), $(-\infty, c)$, and (c_1, c_2), where c, c_1, and c_2 are constants. Parameters defined on half-bounded intervals (such as η^2, λ, and κ) may be log-transformed. Parameters defined on bounded intervals (such as τ and α) may be logit-transformed. In fact, the algorithm below is applicable to any model formulation as long as all the parameters are defined on $(-\infty, \infty)$, either directly or after transformation.

The prior given by (6) is for the parameters on their natural scale. The prior for the transformed parameters are determined by (6) and the transformations. To avoid clutter in notation, we shall still use θ to denote the parameter vector (now transformed) and refer to (6) for its prior, although in reality the prior of the transformed parameter is a modified form of (6). The algorithm actually derives posterior distribution of these *transformed*

parameters. Distribution of the parameters on their natural scale can be studied based on back-transformed samples from the derived posterior distribution.

3.1 Algorithm

We begin with an initial approximation to the posterior, denoted by $f^{(0)}(\theta)$, which is taken to be a sufficiently diffuse multivariate normal distribution. In the kth iteration, the current approximation $f^{(k-1)}$ is updated to $f^{(k)}$ in three steps as follows.

1. Take a random sample, $\{\theta_1, \ldots, \theta_n\}$, from $f^{(k-1)}$.

2. For $i = 1, \ldots, n$, compute the non-normalized posterior density $s_i = \pi(\theta_i)\, p(\boldsymbol{y} \,|\, \theta_i)$ and the proposal density $t_i = f^{(k-1)}(\theta_i)$; let $w_i = \frac{s_i/t_i}{\sum_{j=1}^n s_j/t_j}$ be the importance weight of θ_i.

3. Update the approximate posterior from $f^{(k-1)}$ to

$$f^{(k)}(\theta) \approx \sum_{i=1}^{n} w_i\, \phi(\theta;\, \theta_i, V_i). \tag{7}$$

 This is a mixture of n normal densities (denoted by ϕ), each with mean θ_i and covariance matrix V_i. Computation of V_i is detailed in Section 3.2.

This algorithm does not require one to be able to draw a random sample from the prior of θ. Instead, a convenient initial approximation, $f^{(0)}$, starts the procedure. One only needs to be able to *calculate* the prior density for any particular value of θ. This provides great flexibilities in choosing the prior $\pi(\theta)$ and the initial approximation $f^{(0)}$. Sampling from a normal mixture distribution is easy.

Note that $f^{(k)}$ is a normal mixture, just like $f^{(k-1)}$, and is ready to be updated in the next iteration. Alternatively, one may terminate the iteration according to certain empirical criterion, and take $f^{(k)}$ as the final approximate posterior distribution of the parameter θ.

Some properties of $f^{(k)}$ may be examined semi-analytically. More often, one is more interested in the unknown field Y or a function thereof than in the parameter θ itself. Properties of Y or a function thereof may be investigated via sampling θ from $f^{(k)}(\theta)$ and simulating (i.e. sampling) $\tilde{\boldsymbol{y}}$ (realization of the field) according to (5).

3.2 Algorithm detail: computation of V_i

The step 3 of the algorithm entails kernel density estimation, which is a standard but unsettled task [Silverman, 1986; Scott, 1992; Wand and Jones, 1995]. The covariance matrix V_i may be expressed as $h_i \Sigma_i$, where Σ_i is the empirical weighted covariance matrix of the sample points (θ's) in a certain neighborhood of θ_i, and h_i is a "bandwidth" parameter. While Σ_i specifies the shape of the kernel centered at θ_i, the bandwidth h_i further adjusts the spread of this kernel.

Several factors complicate the computation of V_i. First, the distribution of the importance weights, w_i, can be highly skewed, especially in early iterations when the proposal distribution tends to be very different from the true posterior distribution. In not-so-rare pathological cases, a few sample points (or a single sample point) carry a dominant fraction

of the total weight, making the other sample points negligible. When this happens, Σ_i may contain variance entries that are nearly 0. To mitigate this problem, we use a "flattened" version of weights in the computation of Σ_i. Let

$$v_i = \frac{w_i^\gamma}{\sum_{j=1}^n w_j^\gamma}, \quad \text{where} \quad \gamma = -\frac{1}{\log n} \sum_{i=1}^n w_i \log w_i. \tag{8}$$

The exponent γ is the "entropy" of $\{w_i\}$, a measure of the uniformity of the weights [see West, 1993]. If $\{w_i\}$ are all equal, then $\gamma = 1$. At the other extreme, if one w_i is 1 and all the other weights are 0, then $\gamma = 0$. Note that the weights $\{v_i\}$ are used in calculating the empirical weighted covariance matrix Σ_i; they do not replace the weights $\{w_i\}$ in (7). As the algorithm proceeds in iterations, the importance weights $\{w_i\}$ become more uniform, hence γ becomes closer to 1, and the adjustment to $\{w_i\}$ by the above "flattening" becomes minor.

The second complication is in the "localization" of Σ_i, that is, we choose to define Σ_i as the empirical weighted covariance matrix of sample points in a "neighborhood" of θ_i, say sample points that take up a fraction r_i, $0 < r_i \le 1$, of the entire sample. Such localization is important if the target distribution (i.e. the posterior) is severely multi-modal [Givens and Raftery, 1996]. However, there is no guidance on the determination of the fraction r_i.

The third complication is due to the bandwidth h_i. A number of adaptive procedures have been proposed for choosing h [Jones, 1990; Hall et al., 1991; Sheather and Jones, 1991; Terrell and Scott, 1992; Givens and Raftery, 1996; Sain, 2002]. However, most of the literature in kernel density estimation is developed based on a *random* sample, whereas what we have here is a *weighted* one. In addition, localization, as parameterized by r_i, has received less attention in the literature. Traditional rule-of-thumb choices for the bandwidth parameter [Jones et al., 1996] do not apply directly to a localized algorithm, because the rules are based on analysis of global estimators. A localized algorithm encounters other difficulties, such as edge effects, that do not arise in a global analysis.

To simplify the matter, we use a common bandwidth parameter, denoted by h (where $h > 0$), and a common localization parameter, denoted by r (where $0 < r \le 1$), for all the mixture components. Sensible choices of these two tuning parameters depend on the sample size n, the dimensionality of θ, and characteristics of the target distribution $\pi(\theta)p(\boldsymbol{y} \mid \theta)$. We determine their values by a maximum likelihood cross-validation criterion:

$$(r, h) = \operatorname*{argmax}_{r,h} J(r, h;\, \theta_1, \ldots, \theta_n), \tag{9}$$

where

$$J(r, h;\, \theta_1, \ldots, \theta_n) = \sum_{i=1}^n w_i \log\left(\frac{1}{1 - w_i} \sum_{j \ne i} w_j \, \phi\big(\theta_i;\ \theta_j, h\Sigma_j\big) \right). \tag{10}$$

Note that Σ_j is a function of r, $\{\theta_i\}$, and $\{v_i\}$. In words, J is the usual log likelihood of r and h with respect to the weighted sample $\{\theta_i\}$, except that the density at θ_i is calculated by the mixture density *leaving out* the mixture component centered at θ_i. Leaving out the offending mixture component is key. Otherwise, maximizing J would drive h to be arbitrarily small. The idea above is quite general, and may be extended to determine other tuning parameters.

To reduce the computational cost of this optimization, a combination of discrete search for r and continuous search for h is performed as sketched below.

1. Let $J^* \Leftarrow -\infty$, that is, assign value $-\infty$ to the variable J^*.

2. Let $r \Leftarrow 1$.

 Let $\Theta_1 \Leftarrow \cdots \Leftarrow \Theta_n \Leftarrow \{\theta_1, \ldots, \theta_n\}$.

 Compute the empirical weighted covariance matrix of the entire sample $\{\theta_1, \ldots, \theta_n\}$, using the flattened weights $\{v_i\}$ instead of the original weights $\{w_i\}$. Denote the result by Σ, and let $\Sigma_1 \Leftarrow \cdots \Leftarrow \Sigma_n \Leftarrow \Sigma$.

3. Find h that maximizes (10). Denote the maximizing h by h_* and the achieved maximum J by J_*.

 (This is a univariate optimization problem. Since we have values of Σ_1,..., Σ_n, the parameter r does not appear in the calculation of (10).)

 If $J_* > J^*$, then let $J^* \Leftarrow J_*$, $r^* \Leftarrow r$, $h^* \Leftarrow h_*$, and $\Sigma_i^* \Leftarrow \Sigma_i$ for $i = 1, \ldots, n$.

4. If r is below a pre-specified threshold fraction, say $\frac{1}{8}$, go to step 6. Otherwise, let $r \Leftarrow r/2$ and go to step 5.

5. For $i = 1, \ldots, n$,

 (a) Within the set Θ_i, identify the $\lceil rn \rceil$ closest neighbors of θ_i in the Mahalonobis sense measured by the covariance matrix Σ_i. Update Θ_i to be the set that contains these newly identified neighbors.

 (b) Compute the empirical weighted covariance matrix, Σ_i, based on the sample Θ_i and the corresponding relative weights $\{v_i\}$.

 Go to step 3.

6. Adopt r^* and h^* as the final values for r and h, respectively, and let the V_i in (7) be $h^*\Sigma_i^*$ for $i = 1, \ldots, n$.

 This concludes the search for optimum values of r and h.

The ideas of normal mixture and iterative updating are used by West [1993]. The procedure in West [1993] sets the bandwidth parameter following empirical rules and does not consider localization.

4 Provisions for the "change of support" problem

The data $\boldsymbol{y}$ in (5) are the values of Y at individual locations $\boldsymbol{x}$. This formulation can be easily generalized to use data that are *linear* functions of Y. Let the data vector, denoted by $\boldsymbol{z}$, be expressed as

$$\boldsymbol{z} = \boldsymbol{H}\boldsymbol{y},$$

where $\boldsymbol{y}$ is a n-vector of Y at locations $\boldsymbol{x}$ and $\boldsymbol{H}$ is a $m \times n$ matrix of rank m, where $m \leq n$. Correspondingly, the likelihood (5) is replaced by

$$p(\boldsymbol{z} \,|\, \theta) = (2\pi\eta^2)^{-m/2} \, |\boldsymbol{H}\boldsymbol{R}\boldsymbol{H}^T|^{-1/2} \exp\Big(-\frac{1}{2\eta^2}\big(\boldsymbol{z} - \boldsymbol{H}\boldsymbol{X}\beta\big)^T [\boldsymbol{H}\boldsymbol{R}\boldsymbol{H}^T]^{-1}\big(\boldsymbol{z} - \boldsymbol{H}\boldsymbol{X}\beta\big)\Big), \tag{11}$$

where $\boldsymbol{X}$ is the design matrix for the locations $\boldsymbol{x}$, and $\boldsymbol{R}$ is the correlation matrix between the locations $\boldsymbol{x}$. The algorithm described in Section 3 works for this form of data and likelihood without modification.

In applications, measurements of Y often have areal or volume (or, in 1-D, interval) support rather than point support. Consider studies in which the model domain is discretized into a numerical grid. Let us call the numerical grid the "basic" spatial unit (or support) in the model. It may occur that a data value is some function (e.g. the average) of Y in more than one basic spatial unit. Specifically, we may distinguish "point data", which have the basic support in the model, and "linear data", which have aggregated support and can be expressed as linear functions (such as simple averages) of point data. Increasingly in environmental studies, available data include a mix of satellite- and ground-based measurements that span a hierarchy of spatial supports. This entails the so-called "change of support" problems [Young and Gotway, 2007], a typical example being "downscaling" problems. The method described above is able to use data on a variety of supports as long as they are all *linear* functions of Y on the basic support.

Besides being a natural situation due to data resources on disparate scales, linear data can also be useful by methodological design. For example, Zhang [2011] proposes an inverse algorithm in which a key model device is linear functions of the random field.

5 Examples

We illustrate the algorithm with two examples. The first example uses a satellite elevation dataset to demonstrate the algorithm's performance in a 2-D, anisotropic setting. Because the true field is known in this case, model performance can be assessed by comparing conditional simulations with the true field. The second example uses a historical dataset of soil moisture. In this realistic setting, the true field is unknown, and the sampling locations of the measurements are not ideal as far as interpolation is concerned (as is a common situation with historical data). However, the point of the examples is not to interpolate, but to illustrate how the algorithm works with available data to approximate the posterior distribution of the model parameters in an iterative procedure.

5.1 Example 1

We extracted satellite tomography data from the National Elevation Dataset (NED) on the web site of the National Map Seamless Server operated by the U.S. Geological Survey, EROS Data Center, Sioux Falls, South Dakota. The particular dataset we used covers a region in the Appalachian mountains on a 37×23 grid. The elevation map is shown in Figure 1, which also marks 20 randomly selected locations that provided synthetic measurements.

We modeled the elevation, denoted by $Y(x)$, by the geostatistical formulation described in Section 2 with a linear trend function and geometric anisotropy. The smoothness κ was fixed at 1.5. This formulation has eight parameters: β_0, β_X, β_Y, α, λ_X, λ_Y, η^2, and τ. As mentioned in Section 3, the algorithm works with a transformed parameter vector: $\theta = \left(\beta_0, \beta_X, \beta_Y, \log \frac{\alpha}{\frac{\pi}{2}-\alpha}, \log \lambda_X, \log \lambda_Y, \log \eta^2, \log \frac{\tau}{1-\tau}\right)$. It is straightforward to study the parameters in their natural units by back-transforming samples from the estimated posterior distribution of θ.

Table 1: Convergence of the approximate posterior to the true posterior in iterations of Example 1, as indicated by functions of the importance sampling weights.

iteration (k)	1	2	3	4	5	6	7	8
sample size (n)	3000	2800	2620	2458	2312	2181	2063	1957
entropy (γ)	0.12	0.35	0.37	0.57	0.80	0.88	0.91	0.92
L_1 distance (d_{L_1})	1.99	1.92	1.86	1.68	1.22	1.05	0.88	0.84

The initial approximation $f^{(0)}(\theta)$ was taken to be the product of eight independent and fairly diffuse normal distributions, one for each component of θ. This initial distribution was updated eight times in the iterative algorithm. During the iterations, the approximate posterior, $f^{(k)}$, converged to the true posterior, $\pi(\theta)\, p(\boldsymbol{y} \,|\, \theta)$ (up to a normalizing factor). The convergence was examined via two measures that indicate the "closeness" or "distance" of two distributions.

The first measure is the entropy of importance sampling weights. Consider the sample $\{\theta_i\}_{i=1}^n$ obtained in step 1 (see Section 3.1) of the k-th iteration, which is a random sample from the density $f^{(k-1)}(\theta)$. The entropy of the importance weights $\{w_i\}_{i=1}^n$, obtained in step 2 of the algorithm, is the γ defined in (8). The entropy can be used as an indicator of how close the estimated distribution, $f^{(k-1)}(\theta)$, is to the true posterior distribution. An entropy value close to 1 indicates good approximation [West, 1993; Liu et al., 1998].

The second measure is the L_1 distance between the estimated posterior, say $f(\theta)$, and the true posterior, $cg(\theta) = c\pi(\theta)p(\boldsymbol{y} \,|\, \theta)$, where c is an unknown normalizing constant. The L_1 distance is defined as $L_1 = \int_\Theta |f(\theta) - cg(\theta)| \,\mathrm{d}\theta$, hence

$$\begin{aligned} L_1 &= \int_\Theta \left| 1 - \frac{g(\theta)}{f(\theta) \int_\Theta g(\theta) \,\mathrm{d}\theta} \right| f(\theta) \,\mathrm{d}\theta \\ &= \int_\Theta \left| 1 - \frac{\frac{g(\theta)}{f(\theta)}}{\int_\Theta \frac{g(\theta)}{f(\theta)} f(\theta) \,\mathrm{d}\theta} \right| f(\theta) \,\mathrm{d}\theta \\ &= E_{f(\theta)} \left| 1 - \frac{g(\theta)/f(\theta)}{E_{f(\theta)}\big[g(\theta)/f(\theta)\big]} \right|, \end{aligned}$$

where the two expectations are with respect to the distribution $f(\theta)$. Therefore, a Monte Carlo estimate of this distance is

$$d_{L_1} = \frac{1}{n} \sum_{i=1}^n |1 - n w_i|,$$

making use of the fact that the sample mean of $\frac{g(\theta)}{f(\theta)}$ is $\frac{1}{n}\sum_{i=1}^n w_i$, i.e. $\frac{1}{n}$.

The values of γ and d_{L_1} in each iteration are listed in Table 1, which shows definite trends of increase in γ and decrease in d_{L_1}.

In total we obtained nine approximate posterior distributions, including the initial approximation and the eight subsequent updates. From each of these approximations we drew 1000 samples of the parameter vector θ. The marginal distribution of each component of θ

Table 2: Empirical mean and standard deviation of 1000 samples of the parameters (back-transformed to their natural units) drawn from the final posterior approximation in Example 1.

parameter	β_0	β_X	β_Y	λ_X	λ_Y	α	η^2	τ
sample mean	941	-9.01	0.81	36.1	2.90	0.32	4.95e04	0.06
sample s.d.	168	4.67	11.6	30.7	2.15	0.08	7.12e04	0.09

is plotted in Figure 2. It can be seen that the posterior approximations stabilized after six or seven iterations, consistent with the quantitative indicators in Table 1. The stabilized approximate distributions of the scale, variance, and nugget parameters are more outspread than those of the trend and rotation parameters. This is related to the interactions between the former group of parameters, which cause identifiability difficulties [see Zhang, 2004].

To provide some idea of the posterior mean and uncertainty of the individual parameter components, Table 2 lists the empirical means and standard deviations of the eight parameter components calculated using the 1000 samples from $f^{(8)}(\theta)$, the final approximation. The empirical posterior mean of the rotation, α, is 0.32, i.e. 18 degrees. The empirical posterior mean of the scale along the rotated horizontal axis (λ_X) is 36.1, in contrast to 2.90 along the vertical axis. The angle and scales are in keeping with what we observe in the synthetic true field. We note that, with the 20 irregularly located measurements in this example, these anisotropy parameters would be difficult to estimate by methods based on curve-fitting for empirical variograms [see, e.g. Paleologos and Sarris, 2011].

In geostatistical analysis, one of the usual goals is to provide an interpolated map of the spatial field accompanied by a measure of uncertainty. We conducted 100 conditional simulations based on the final approximation to the posterior distribution of the parameter. The point-wise median of the simulations is shown in Figure 3. A comparison of Figure 3 with Figure 1 confirms that the model and algorithm have captured main features of the true spatial field. The point-wise standard deviation of the simulations is shown in Figure 4. The level of uncertainty in the simulated fields is largely uniform throughout the model domain, because the locations of the observations are reasonably balanced in the model domain.

5.2 Example 2

In the second example, we used a hydrologic dataset provided by the Southeast Watershed Research Laboratory (SEWRL) of the U.S. Department of Agriculture. The dataset contains long-term records of a number of hydrologic variables for the Little River Experimental Watershed in south-central Georgia, United States. This research program as well as its data products are described in Bosch et al. [2007a]. For illustration, we focused on a time snapshot (specifically, at 18:00 on 1 August 2007) of soil moisture represented by measurements at 29 irregularly-located gauges. The measurements are shown in Figure 5. Details about the regional geography and the moisture data can be found in Bosch et al. [2007a] and Bosch et al. [2007b], respectively.

Because soil moisture is a percentage, we took its logit transform as the spatial variable Y, that is, $Y = \log \frac{\text{moisture}}{0.5-\text{moisture}}$. (The upper bound was taken to be 0.5 because it was noticed

Table 3: Convergence of the approximate posterior to the true posterior in iterations of Example 2, as indicated by functions of the importance sampling weights.

iteration (k)	1	2	3	4	5
sample size (n)	2000	1880	1772	1675	1587
entropy (γ)	0.47	0.92	0.98	0.98	0.99
L_1 distance (d_{L_1})	1.82	0.87	0.40	0.36	0.31

Table 4: Empirical mean and standard deviation of 1000 samples of the parameters (back-transformed to their natural units) drawn from the final posterior approximation in Example 2.

parameter	β	λ	η^2	τ
sample mean	-0.78	30897	0.52	0.21
sample s.d.	0.39	56140	0.41	0.16

that the largest observed value is 0.34.) Such a transformation is needed because Y must be defined on $(-\infty, \infty)$ in order to be modeled as a Gaussian variable. This treatment is in line with generalized linear models in model-based geostatistics [Diggle and Ribeiro Jr., 2007]; but see Michalak and Kitanidis [2005] for an alternative approach.

With the parameterization described in Section 2, we took the trend model $\mu(x)^T\beta$ to be a constant β, fixed the smoothness parameter κ at 0.5 (i.e. used an exponential correlation function), and did not consider anisotropy. This left us with four parameters: β, η^2, λ, and τ. The algorithm worked with a transformed parameter vector: $\theta = \left(\beta, \log\eta^2, \log\lambda, \log\frac{\tau}{1-\tau}\right)$.

Construction of the prior and the initial approximate posterior distributions followed procedures similar to those in the first example. The initial distribution was updated five times. The convergence of the approximate posterior distributions to the truth were examined via the two measures γ and d_{L_1} as listed in Table 3. The values listed show definite trends of increase in γ and decrease in d_{L_1}. As γ and d_{L_1} approached their respective limits, 1 and 0, their values began to "level off".

Table 4 lists the empirical means and standard deviations of the four parameter components obtained using 1000 samples from the final posterior approximation.

A major purpose of a geostatistical analysis like the current one is to generate an ensemble of soil moisture maps to be used in subsequent studies that require the value of soil moisture in the entire domain. We divided the model domain into 41 (east-west) by 74 (north-south) grids, each of size 1106 m $\times$ 1106 m, and conducted 100 conditional simulations based on the approximate posterior distribution obtained in the final iteration of the algorithm. Each simulation was back-transformed to give a moisture map with values in $(0, 0.5)$, in contrast to the variable $Y \in (-\infty, \infty)$ in the model. The point-wise median of the simulations is shown in Figure 6, which confirms a high-moisture area in the upper-central section of the model domain. More scientific insights are expected if one examines the simulated soil moisture maps in the context of other hydrologic variables as well as the geography.

6 Conclusion

We have described a Bayesian geostatistical framework and proposed an iterative algorithm for deriving the posterior distribution of the parameter vector. The contribution of this study is to provide a general inference procedure that avoids some difficult elements utilized in practice, including (1) fitting a variogram curve; (2) imposing bounds on an unbounded parameter; (3) discretizing a continuous parameter. Moreover, the procedure can be applied to other model formulations as long as the model parameters, or transforms thereof, are defined on $(-\infty, \infty)$. Common transformations that achieve this goal include the logarithmic and logistic transformations, as exemplified in Section 5.

The algorithm centers on normal kernel density estimation. Particular efforts are made to determine the localization and bandwidth parameters in a systematic fashion. Difficulties caused by highly skewed importance sampling weights are alleviated by "flattening" the weights.

The method was demonstrated by two examples using synthetic and historical data. In both examples, we examined convergence of the approximate posterior distributions, as well as features of the marginal posterior distributions. The estimated posterior distributions served as a basis for conditional simulations of the spatial field.

Acknowledgement: The author's Senior Visiting Scholarship at Tsinghua University was funded by the Excellent State Key Lab Fund no. 50823005, National Natural Science Foundation of China, and the R&D Special Fund for Public Welfare Industry no. 201001080, Chinese Ministry of Water Resources.

References

M. Abramowitz and I. A. Stegun, editors. *Handbook of Mathematical Functions*. Dover, New York, 1965.

S. Banerjee, B. P. Carlin, and A. E. Gelfand. *Hierarchical Modeling and Analysis of Spatial Data*. Chapman & Hall/CRC, 2004.

J. O. Berger, V. De Oliveira, and B. Sansó. Objective Bayesian analysis of spatially correlated data. *J. Am. Stat. Assoc.*, 96(456):1361–1374, 2001.

D. D. Bosch, J. M. Sheridan, R. R. Lowrance, R. K. Hubbard, T. C. Strickland, G. W. Feyereisen, and D. G. Sullivan. Littel River Experimental Watershed database. *Water Resour. Res.*, 43:W09470, 2007a. doi: 10.1029/2006WR005844.

D. D. Bosch, J. M. Sheridan, and L. K. Marshall. Precipitation, soil moisture, and climate database, Little River Experimental Watershed, Georgia, United States. *Water Resour. Res.*, 43:W09472, 2007b. doi: 10.1029/2006WR005834.

O. F. Christensen, P. J. Diggle, and P. J. Ribeiro Jr. Analysing positive-valued spatial data: the transformed Gaussian model. In P. Monestiez, D. Allard, and R. Froidevaux, editors, *geoENV III—Geostatistics for Environmental Applications*, pages 287–298. Kluwer, 2001.

M. K. Cowles, J. Yan, and B. Smith. Reparameterized and marginalized posterior and predictive sampling for complex Bayesian geostatistical models. *J. Comp. Graph. Stat.*, 18(2):262–282, 2009. doi: 10.1198/jcgs.2009.08012.

V. de Oliveira, B. Kedem, and D. A. Short. Bayesian prediction of transformed Gaussian random fields. *J. Am. Stat. Assoc.*, 92(440):1422–1433, 1997.

P. J. Diggle and P. J. Ribeiro Jr. Bayesian inference in Gaussian model-based geostatistics. *Geographical & Environmental Modelling*, 6(2):129–146, 2002.

P. J. Diggle and P. J. Ribeiro Jr. *Model-based Geostatistics*. Springer, 2007. ISBN 0-387-32907-2.

M. D. Ecker and A. E. Gelfand. Bayesian modeling and inference for geometrically anisotropic spatial data. *Math. Geol.*, 31(1):67–83, 1999.

X. Emery. Reducing fluctuations in the sample variogram. *Stoch. Environ. Res. Risk Assess.*, 21:391–403, 2007.

A. Gelman. Prior distributions for variance parameters in hierarchical models. *Bayesian Analysis*, 1(3):515–533, 2006.

A. Gelman, J. B. Carlin, H. S. Stern, and D. B. Rubin. *Bayesian Data Analysis*. Chapman & Hall/CRC, 2nd edition, 2004.

G. H. Givens and A. E. Raftery. Local adaptive importance sampling for multivariate densities with strong nonlinear relationships. *J. Am. Stat. Assoc.*, 91(433):132–141, 1996.

P. Hall, S. J. Sheather, M. C. Jones, and J. S. Marron. On optimal data-based bandwidth selection in kernel density estimation. *Biometrika*, 78(2):263–269, 1991.

M. S. Handcock and M. L. Stein. A Bayesian analysis of kriging. *Technometrics*, 35(4): 403–410, 1993.

D. T. Hristopulos. New anisotropic covariance models and estimation of anisotropic parameters based on the covariance tensor identity. *Stoch. Environ. Res. Risk Assess.*, 16:43–62, 2002.

M. C. Jones. Variable kernel density estimates and variable kernel density estimates. *Austral. J. Statist.*, 32(3):361–371, 1990.

M. C. Jones, J. S. Marron, and S. J. Sheather. A brief survey of bandwidth selection for density estimation. *J. Am. Stat. Assoc.*, 91(433), 1996.

P. K. Kitanidis. Parameter uncertainty in estimation of spatial functions: Bayesian analysis. *Water Resour. Res.*, 22(4):499–507, 1986.

J. L. Kovitz and G. Christakos. Spatial statistics of clustered data. *Stoch. Environ. Res. Risk Assess.*, 18:147–166, 2004.

J. S. Liu, R. Chen, and W. H. Wong. Rejection control and sequential importance sampling. *J. Am. Stat. Assoc.*, 93(443):1022–1031, 1998.

J. S. Marron and M. P. Wand. Exact mean integrated squared error. *Ann. Statist.*, 20(2): 712–736, 1992.

A. M. Michalak and P. K. Kitanidis. A method for the interpolation of nonnegative functions with an application to contaminant load estimation. *Stoch. Environ. Res. Risk Assess.*, 19:8–23, 2005.

M. B. Palacios and M. F. J. Steel. Non-Gaussian Bayesian geostatistical modeling. *J. Am. Stat. Assoc.*, 101:604–618, 2006.

E. K. Paleologos and T. S. Sarris. Stochastic analysis of flux and head moments in a heterogeneous aquifer system. *Stoch. Environ. Res. Risk Assess.*, 25:747–759, 2011.

S. R. Sain. Multivariate locally adaptive density estimation. *Computational Statistics & Data Analysis*, 39(2):165–186, 2002.

D. W. Scott. *Multivariate Density Estimation*. John Wiley & Sons, Inc., 1992.

S. J. Sheather and M. C. Jones. A reliable data-based bandwidth selection method for kernel density estimation. *J. R. Stat. Soc., B*, 53(3):683–690, 1991.

B. W. Silverman. *Density Estimation for Statistics and Data Analysis*. Chapman & Hall, 1986.

M. L. Stein. *Interpolation of Spatial Data: Some Theory for Kriging*. Springer, 1999.

G. R. Terrell and D. W. Scott. Variable kernel density estimation. *Ann. Statist.*, 20(3): 1236–1265, 1992.

H. Wackernagel. *Multivariate Geostatistics*. Springer-Verlag, Berlin, 3rd edition, 2003. ISBN 3-540-44142-5.

M. P. Wand and M. C. Jones. *Kernel Smoothing*. Chapman & Hall/CRC, 1995.

J. J. Warnes and B. D. Ripley. Problems with lieklihood estimation of covariance functions of spatial Gaussian processes. *Biometrika*, 74(3):640–642, 1987.

M. West. Approximating posterior distributions by mixture. *J. R. Stat. Soc., B*, 55(2): 409–422, 1993.

L. J. Young and C. A. Gotway. Linking spatial data from different sources: the effects of change of support. *Stoch. Environ. Res. Risk Assess.*, 21:589–600, 2007. doi: 10.1007/s00477-007-0136-z.

H. Zhang. Inconsistent estimation and asymptotically equal interpolations in model-based geostatistics. *J. Am. Stat. Assoc.*, 99(465), 2004. doi: 10.1198/016214504000000241.

Z. Zhang. Adaptive anchored inversion for Gaussian random fields using nonlinear data. *Inverse Problems*, 27(12):125011, 2011. doi: 10.1088/0266-5611/27/12/125011.

D. L. Zimmerman. Another look at anisotropy in geostatistics. *Math. Geol.*, 25(4):453–470, 1993.

D. L. Zimmerman. Likelihood-based methods. In A. E. Gelfand, P. J. Diggle, M. Fuentes, and P. Guttorp, editors, *Handbook of Spatial Statistics*, chapter 4. CRC Press, 2010.

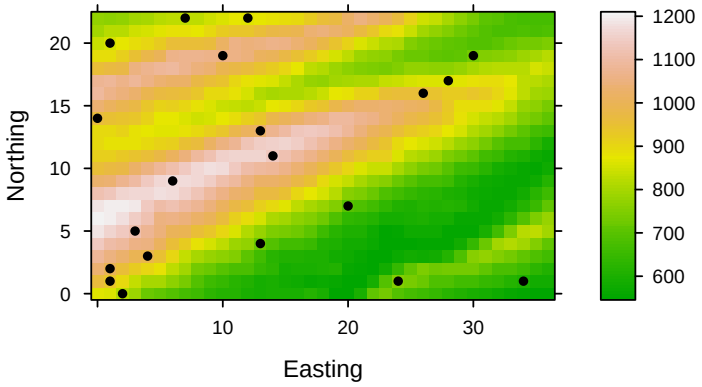


Figure 1: Elevation map as the synthetic true field for the example in Section 5.1. The 20 dots indicate synthetic measurements.

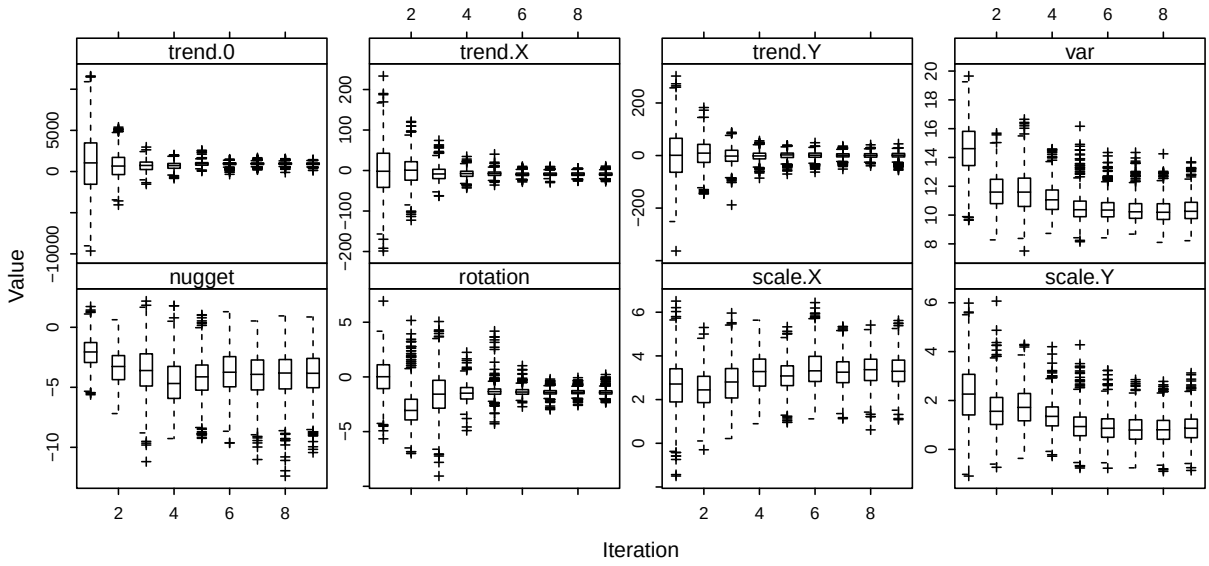


Figure 2: Marginal distributions (by boxplots) of the model parameters as revealed by 1000 samples drawn from each of the 8 iterative approximations to the posterior distribution. The parameters are in transformed units, hence taking values on $(-\infty, \infty)$. See Section 5.1.

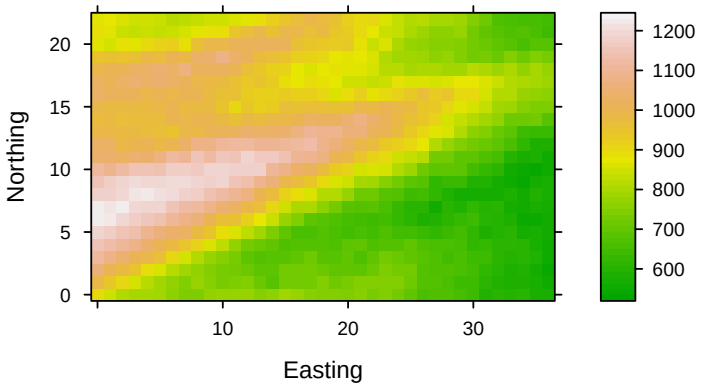


Figure 3: Point-wise median of 100 simulations conditional on model parameters drawn from the final approximation to the posterior distribution. See Section 5.1.

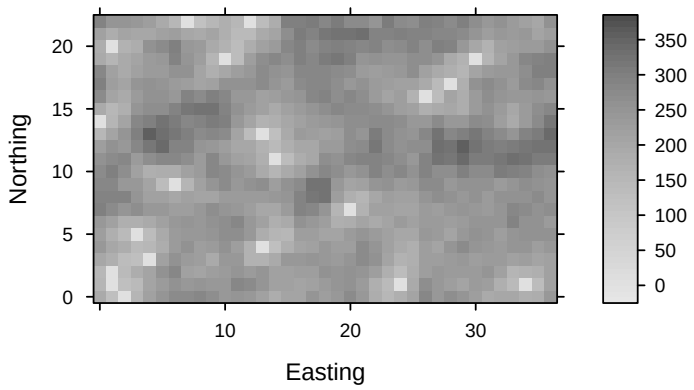


Figure 4: Point-wise standard deviation of 100 simulations conditional on model parameters drawn from the final approximation to the posterior distribution. Note that variation at the locations of the 20 measurements is 0. See Section 5.1.

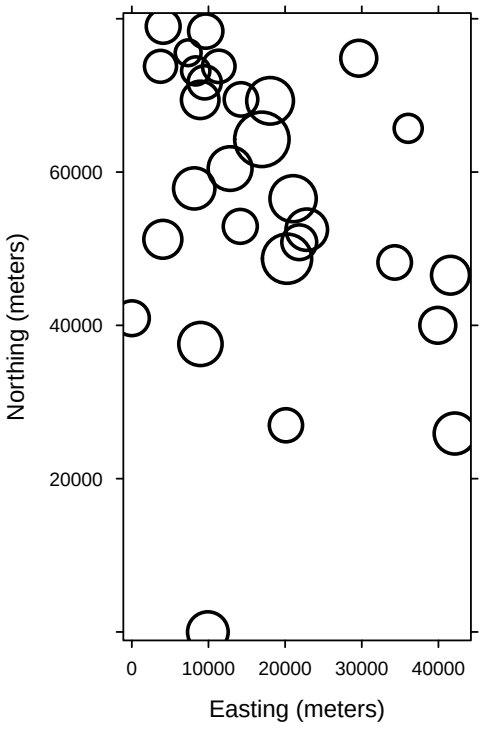


Figure 5: Locations of 29 soil moisture measurements (cm^3/cm^3) for the example in Section 5.2. Areas of the circles are proportional to the moisture values.

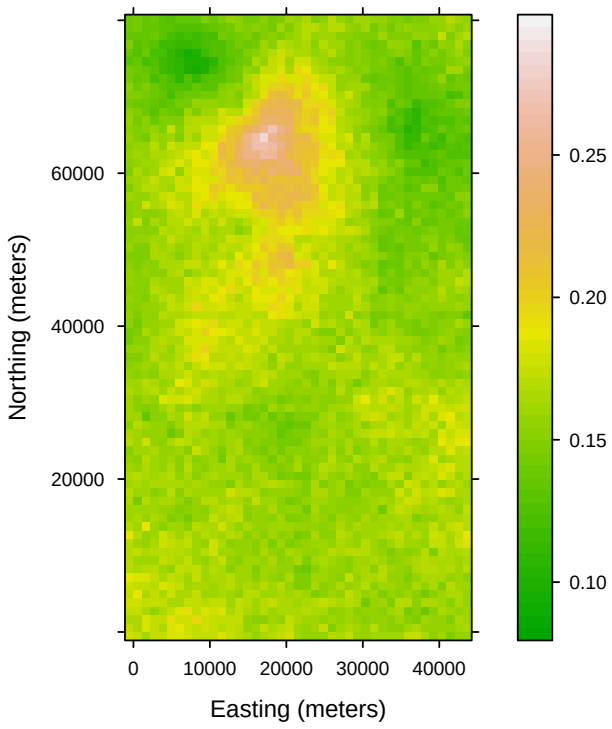


Figure 6: Point-wise median of 100 simulations conditional on model parameters drawn from the final approximation to the posterior distribution. See Section 5.2.